Laura Naujokaitytė,
Eugenija Strazdienė,
Jurgita Domskienė

Kaunas University of Technology
Faculty of Design and Technologies
Department of Clothing
and Polymer Product Technology
Studentų str. 56
LT-51424 Kaunas
Lithuania
Phone: +370 65 200 353
Faxe: +370 37 353 989
E-mails: Laura.Naujokaityte@stud.ktu.lt
Eugenija.Strazdiene@ktu.lt
Jurgita.domskiene@ktu.lt

Investigation of Fabric Behaviour in Bias Extension at Low Loads

Abstract
Shear deformations are the most significant mode of deformation during draping or forming processes. The bias extension test can be used to trace the parameters describing fabric shear. In this research the image analysis method in combination with an bias extension test were used for characterisation of the specimen buckling point and surface irregularity changes during uni-axial extension. Buckling point dependence on stiffener concentration was recorded. Shear angle values were obtained by an optical method. Particular focus was placed on the methods capability to distinguish fabrics of similar structure and those that differ in the bending rigidity parameter, which is changed by the PVA stiffener concentration. Shear angle dependence on the load and extension is presented. Shear parameters obtained from the bias extension test were proved to correlate with the shear parameters obtained by well known methods.

Key words: *shear, critical shear angle, bias extension, buckling, image analysis.*

Introduction

The suitability of fabrics for tailoring and the quality of garment appearance is related to certain mechanical properties of the fabric. During the manipulation of a fabric, internal stresses and strains are induced within it. Fabrics undergo a complex combination of deformations like extension, longitudinal compression, bending and shear. The shearing behaviour of fabrics is of the utmost importance to fabric producers, garment manufacturers and the composite industry. It plays a crucial role in fabric formability when doubly curved surfaces must be covered. The ability of fabric to shear within a plain enables it to fit three-dimensional surfaces without folds [1, 2].

There are three basic principles for shear investigation [3-5]. The first method involves a fabric being clamped along two opposite edges and sheared by moving one of the clamped edges at a constant speed. During shear, the clamped edges are kept apart by a tension. This is the operating principle in KES-F, which is also usually applied to manually determine the 'shear lock angle' of fabrics. The second type of shear apparatus involves a square textile sample held within a picture frame. Two diagonally opposite corners of the picture frame are pulled apart at a constant rate. If it is assumed that the fabric is inextensible, there is only in-plain shear before wrinkling starts. The third group of methods for testing shear employs the bias extension principle. It has been proved by various authors [6-8] that shear rigidity can be calculated from the tensile properties along a 45° bias direction. Bias extension tests are simple to perform and provide reasonably repeatable results. This method is functional in shear lock angle estimation as well.

When the shear locking angle is reached and the threads are physically jammed up, buckling occurs and woven fabrics undergo 'in plane' (tensile and shear) and 'out of plain' (bending) deformations [9, 10].

Various image analysis systems are widely applied for investigation of fault features, the abrasion behaviour of yarns, for the investigation of non-woven basis weight, for the fiber length distribution in nonwovens, for the investigation of fabric pilling properties and for the assessment of wrinkling, which is widely used. Digital image processing of images of textile products mainly involves the computer processing of 2D-images, which includes image acquisition, modelling (digitising the real image), as well as image quality improvement and highlighting its distinguishing features [11].

When viewed under certain lightning conditions, a flat plain fabric appears as an area of uniform light intensity, whereas in the case of wrinkled plain fabric, it appears as a set of regions of different light intensities. The magnitude of intensities depends on the level of wrinkles and on the illumination conditions. If constant conditions of illumination can be assured, the comparison of surface irregularities between different fabrics can be done [12]. An image analysis method based on these considerations was proved by J. Domskiene *et al*. [13] to be applicable for the determination of the critical shear angle of fabrics and for the investigation of fabric surface buckling during uniaxial tension. In [13] the method was proved to show some peculiarities of shear and buckling behaviour for the fabrics relatively different in structure and properties.

The present paper focuses on the applicability of the bias extension method for further investigation of the shear and buckling behavior of fabrics of similar structure but varying in certain mechanical parameters i.e. bending rigidity, which was changed by applying different stiffener treatments. The scope of the investigation was to trace the buckling point on the load-deformation curve, to find its dependence on the concentration of the stiffener, to investigate the propagation of surface irregularities during bias extension using an image analysis method, to explore the dependence of the shear angle on the load and extension and to compare the shear parameters obtained from the bias extension test with well known methods.

Experimental

100% cotton fabric was chosen for the investigation, and four different finishing treatments were applied to the test samples in order to change the bending rigidity parameter. These four groups of fabrics were obtained by treating pieces of fabric with PVA (polyvinyl acetate) stiffener dispersions in water concentrations differing by 5 ml/l (i.e. untreated samples and those treated with 5 ml/l, 10 ml/l and 15 ml/l stiffener concentrations). The specifications of the samples and the coefficient of bending rigidity B in μN·m obtained according to the FAST cantilever testing method are presented in ***Table 1*** (see page 60). In the cantilever test method, 10 replicate measurements of the bending length were taken with

the variation coefficient $v = 2 – 4\%$, and the bending rigidity was calculated according to equation $B = wc^3 \times 9.81 \cdot 10^{-6}$, where w – area density, c – half of the bending length.

45° bias cut specimens of 50 × 100 mm size were tested on an extensometer in a low load region (six replicate measurements with each fabric). The shear properties were investigated by increasing the load by 4 N/m till the critical shear angle was reached. When the critical shear angle was reached at small loads, further buckling propagation analysis was performed at low stress limits by increasing the load by 10 to 20 N/m till a 200 N/m load was reached. At each increment of load deformation recorded, grayscale digital images of 256 levels and 2592 × 1944 pixel size were captured. For image acquisition a high-resolution digital camera was used. The scheme of the experiment is presented in ***Figure 1.***

A luminescence light source 2 (see ***Figure 1***) of 20W intensity was placed on the same plane as the specimen 1, and the lightning angle was adjusted to maximise the contrast in the image. The lens of camera 3 coincided with the centre of the specimen 1.

Table 1. *Specifications of tested materials.*

Fabric code	Content	Weave type	Yarn density, cm^{-1}		Area density, g/m^2	Treatment	Thickness, mm	Bending rigidity μN·m
			Warp	Weft				Bias
Co_0	100% cotton	Plain	23.6	23.2	137.8	–	0.43	9.77
Co_5					138.1	5 ml/l PVA	0.43	23.18
Co_10					138.5	10 ml/l PVA	0.43	38.76
Co_15					142.0	15 ml/l PVA	0.43	49.70

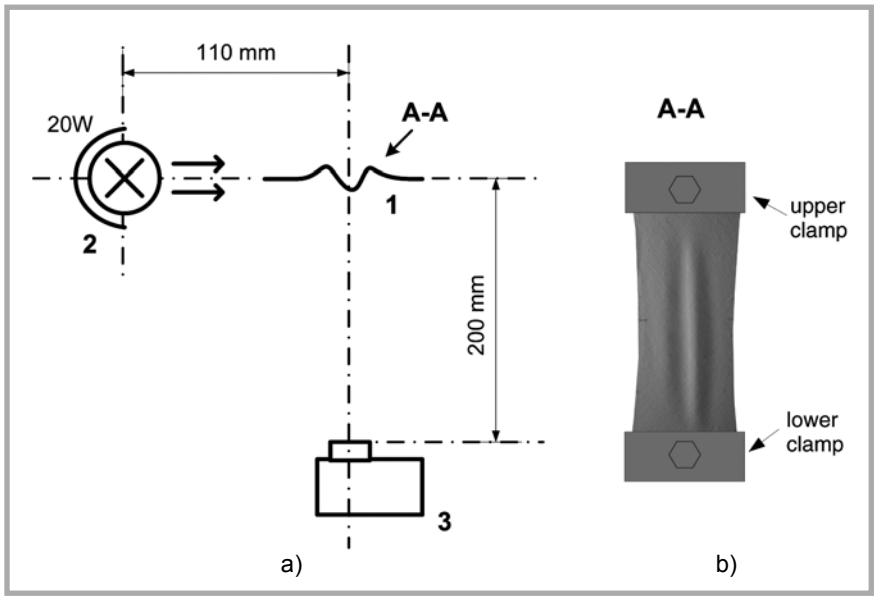

Figure 1. *a – scheme of the experiment: 1 – specimen, 2 – light source, 3 – digital camera; b – frontal view of the specimen.*

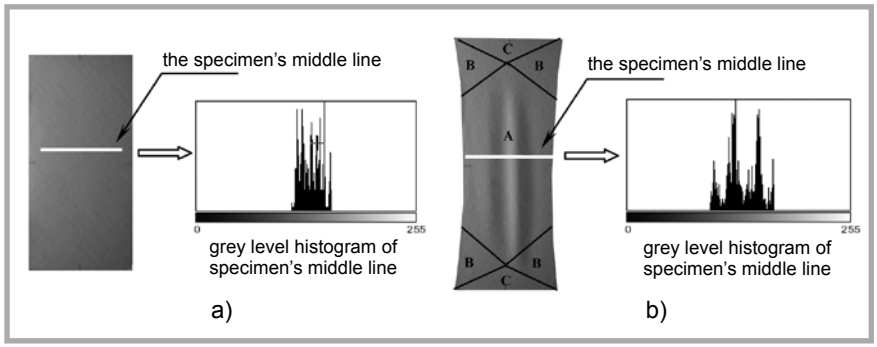

Figure 2. *Analysis of specimen's surface: a – histogram of specimen's middle line in initial state, b – histogram of the specimens middle line in deformed state.*

As revealed in previous experimental studies [5, 9, 14, 15] three distinct zones of a bias stretched woven fabric can be distinguished (see ***Figure 2.b***). The length of the material sample must be at least twice its width in order for three regions of different deformation to exist [15]. Zone A is the square or hexagonal middle part of the specimen where full shear (trellis) deformation occurs, while zones B and C are triangular areas representing no deformation zone (C) and transition region (B), which experiences half the shear deformation of zone A [9, 15]. Thus the analyses of buckling propagation were performed according to the image analysis method described in [13], and the surface waviness was evaluated by calculating the dispersal of the grayscale level *CV* according to Equation 1 in the middle line of centre part A of the specimen (see ***Figure 2***), where the pure shear is observed and the biggest deformations take place.

$$CV = \frac{s}{\bar{I}} \tag{1}$$

Where s – is the standard deviation and $\bar{I}$ – mean value of the grey scale level, which is taken from the plot profile and histogram of the line analysed line. Flatter surfaces generally exhibit a higher mean intensity with a lower variance, while the variance of a wrinkled surface is higher (see ***Figure 2***).

The high resolution of captured images enabled to measure the shear angle directly from the image (see ***Figure 3***) with an accuracy of ± 0,1°.

The shear angle γ was obtained taking five measurements at the central area of the specimen and calculated as an average value:

$$\gamma = \frac{\sum (90° - \theta_i)}{5} \tag{2}$$

From the bias extension test, the shear modulus *G (FAST)* was calculated according to the *FAST* method using the formula $G = 123/E5$, where E5 – is the specimen extension on the bias at a load of 5 N/m.

In order to compare the results obtained in the bias extension test, the widely used Kawabata Evaluation System (KES-FB1) [16] was chosen to obtain the shear modulus *G (KES)* of the fabrics investigated . Three replicate measurements were made in warp and weft directions, and variation coefficients v = 3÷8% were obtained.

***Table 2.** Shear rigidity values obtained by different test methods.*

	CO_0	CO_5	CO_10	CO_15
G (FAST), N/m	66.97	117.14	129.13	153.11
G (KES), N/m·°	2.19	2.79	4.45	4.49

The shear rigidity values obtained by KES-FB according to the FAST standard method are presented in ***Table 2***.

Results and discussion

Stress-strain curves were obtained from the low load bias extension test. The low load region of load-extension curves, where the buckling of a bias stretched specimen starts, is presented in ***Figure 4***. The experimental points marked with circles in ***Figure 4*** specify the limit of in-plain deformation after which a sample starts to show out-of-plane deformation.

The buckling point is described by critical load P_{kr} and critical extension ε_{kr}.

From ***Figure 4*** it is seen that with an increase in stiffness, the ability of fabric to support compressive stresses increases, and the buckling point moves upwards i.e. buckling starts at higher loads, which could be explained by the increased friction among yarns and bigger extensions. Critical load P_{kr} and critical extension ε_{kr} values follow a linear tendency with increasing stiffener concentration (see ***Figure 5***). It is worth mentioning that with increasing values of critical extension, stiffness increases quite markedly from 2.19% for 0 ml/l concentration to 5.63% for 15 ml/l concentration.

For the investigation of surface buckling propagation using the image analysis method, dependencies between the dispersal of the grayscale level *CV* and load are presented in ***Figure 6***. The *CV* vs. extension curves are given in ***Figure 7***.

During the first steps of loading, only in-plane specimen deformations take place; this way the dispersal of the grey scale level *CV* prior to buckling is of a constant value – the specimen surface is plain. In ***Figures 6 and 7*** *CV* variations are presented after the critical shear angle is reached – post fabric buckling behaviour is investigated. With increasing deformation an increase in surface irregularities is observed, and buckling waves get deeper, causing a rise in the value of the disper-

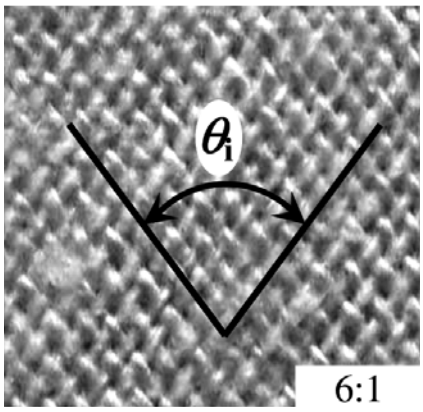

***Figure 3.** Shear angle measurement.*

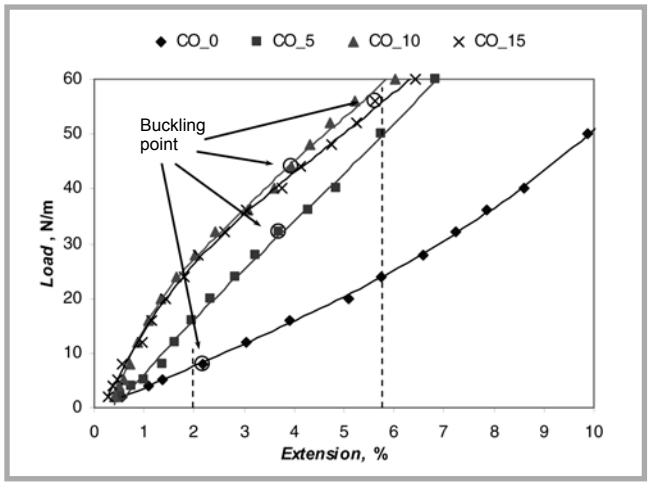

***Figure 4.** Load-extension curve at small loads.*

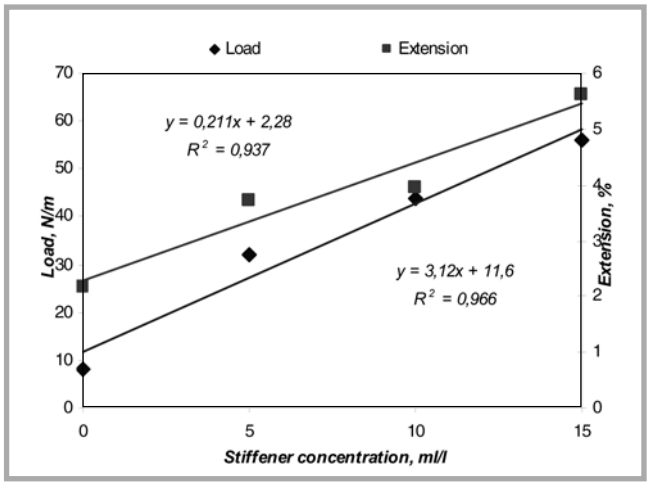

***Figure 5.** Dependence of critical load and extension on stiffener concentration.*

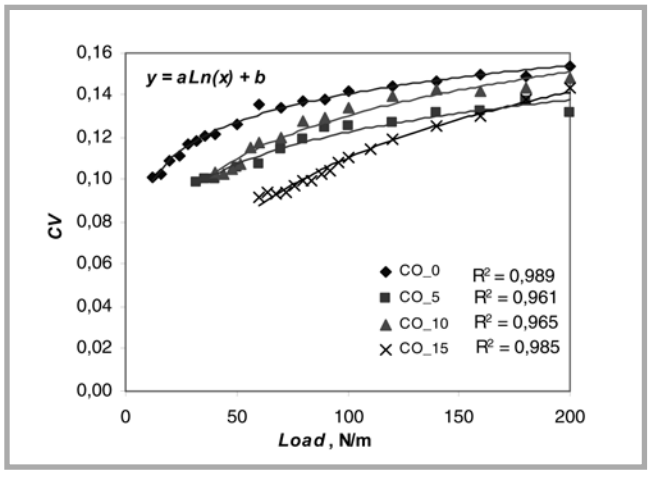

***Figure 6.** Surface irregularities dependence on load.*

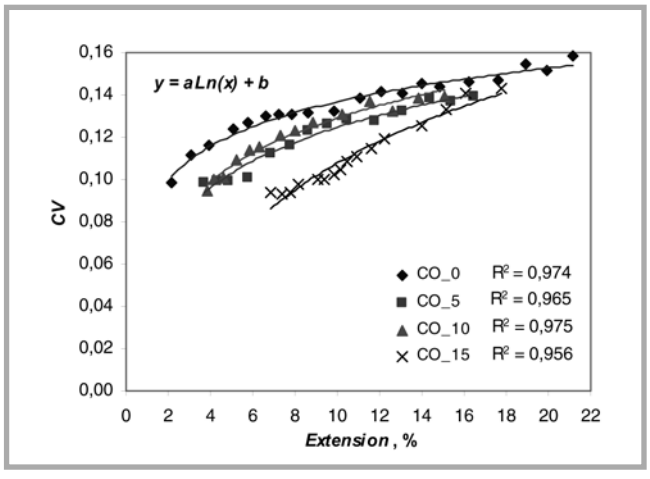

***Figure 7.** Surface irregularities dependence on specimens elongation.*

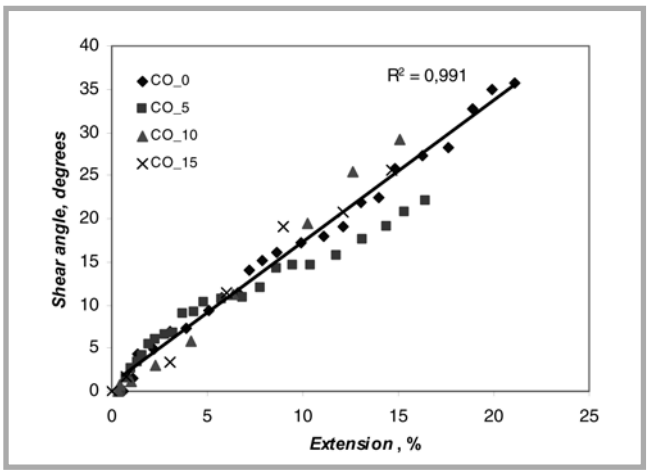

Figure 8. *Shear angle γ change increasing extension ε.*

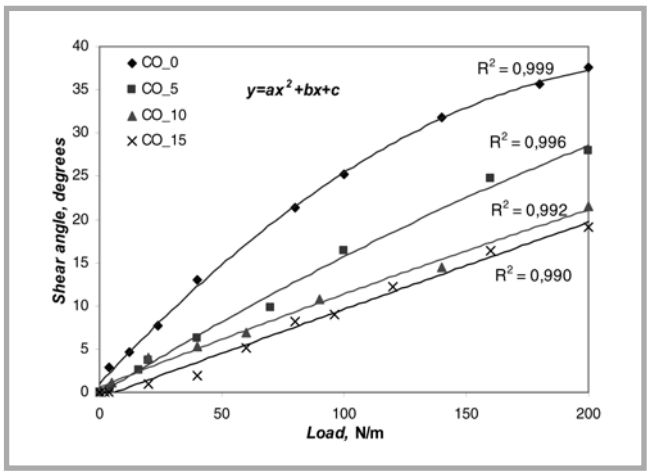

Figure 9. *Shear angle γ dependence on extension load P.*

sal of the grey scale level *CV*. The post-buckling behaviour shown in ***Figures 6 and 7*** follow logarithmic tendencies (see ***Table 3***). Even though in both figures the results obtained with samples of mediate concentration (5 ml/l and 10 ml/l of the stiffener) do not show a clear distinction and fall into the margins of error (± 0.1), the limiting concentrations of 0 ml/l and 15 ml/l show a different behavior, confirming that out-of-plain post-buckling behaviour is influenced by bending rigidity changes that can be determined by the image analysis of captured digital images. The distinction is highest at lower loads, and when it reaches 150 N/m, it starts to fall into the margins of error (± 0.1). In the case of *CV* vs. the extension, the difference becomes intangible when 15 % elongation is reached.

Table 3. *Coefficients a, b of logarithmic function and determination coefficient R^2.*

Fabric code	a	b	R^2
CV vs. Load			
CO_0	0.0193	0.0516	0.989
CO_5	0.0220	0.0215	0.961
CO_10	0.0296	-0.0060	0.965
CO_15	0.0448	-0.0957	0.985
CV vs. Extension			
CO_0	0.0230	0.0838	0.974
CO_5	0.0312	0.0528	0.965
CO_10	0.0326	0.0540	0.975
CO_15	0.0572	-0.0241	0.956

Table 4. *Coefficients a, b, c of polynomial function and determination coefficient R^2.*

Fabric code	a	b	C	R^2
CO_0	-0.0006	0.3073	0.9709	0.999
CO_5	-0.0002	0.1752	-0.2296	0.996
CO_10	$-5 \cdot 10^{-5}$	0.1131	0.6027	0.992
CO_15	$-6 \cdot 10^{-6}$	0.1027	-0.6130	0.990

The shear angle change vs. the extension is plotted in ***Figure 8***. In all the four cases, it was found that in a region of small deformation (up to 20%), in spite of increasing stiffness (i.e. increasing stiffener concentration), the shear angle change showed a similar linear behaviour with increasing extension, except the critical shear angles γ_{cr}, which were reached at higher extensions for stiffer fabrics. In reality, due to compression, compaction and friction wrinkles usually occur well before the locking angle is reached; however, the shear still predominates the deformation mode as well as wrinkling [17]; therefore in our case γ_{cr} is referred to as the shear angle where the buckling starts.

Dependencies between shear angles and the load are presented in ***Figure 9*** (see also ***Table 4***). While increasing the load shear angle was changing according to the second order polynomial dependency. Stiffer fabrics reach the same shear angle at higher loads. Increasing the stiffener concentration in steps of 5 ml/l, the highest load difference at the same shear angle is obtained between concentrations of 0 ml/l and 5 ml/l , in this case the load increased by approximately 2.3 times. With increasing stiffener concentration, the increasing tendency of the load at the same shear angle decreases by 1.4 times between concentrations of 5 ml/l and 10 ml/l and by 1.2 times between 10 ml/l and 15 ml/l.

The values of critical parameters extracted from the bias extension test i.e. the critical load P_{kr}, critical extension ε_{kr} and critical shear angle γ_{cr} are presented in a ***Table 5***.

It is seen that all critical parameters increase with increasing stiffener concentration; however the critical shear angle is smaller in the case of the untreated sample (0 ml/l) and has nearly the same value for the rest of the concentrations (5 ml/l, 10 ml/l and 15 ml/l). This could be explained that after applying different finishing treatments, the bending rigidity properties of the fabric changed, but the basic cell geometry, i.e. macro pores between the threads that are the most responsible for the critical shear angle remained unaltered.

During the bias extension test, out-of-plain buckling was observed. Its occurrence depends on the balance between the membrane and bending strain energies. These two characteristics describe fabric resistance to shear and bending. Thus the dependence between the critical buckling force P_{kr} and shear modulus G as well as the bending rigidity coefficient B is obvious. These considerations were proved by good correlation coefficients between the parameters that are presented in ***Table 6***. Additionally, a comparison was made between the shear modulus obtained using the worldwide accepted standard testing system KES-FB1 and that obtained in the bias extension test (see ***Table 6***).

Good correlation results (r = 0.999) of the shear modulus calculated according to the FAST standard method and measured by KES – FB1 were obtained (see ***Table 5***), although these two testing systems employ different measuring principles.

Conclusions

Small stiffness variations do influence the behaviour of bias cut fabrics during

Table 5. *Values of critical parameters from the bias extension test.*

	CO_0	CO_5	CO_10	CO_15
P_{kr}, N/m	8.00	32.0	44.0	56.00
ε_{kr}	2.19	3.71	3.95	5.63
γ_{cr}, degrees	4.8	6.6	6.8	7.0

Table 6. *Correlation coefficient r between certain mechanical parameters.*

	G (FAST), N/m	B (FAST), μN·m	ε_{kr}	G (FAST), N/m·°
P_{kr}, N/m	0.922	0.987	0.951	0.922
G (FAST), N/m	–	0.965	0.806	0.999

uni-axial tension at low loads. The stiffer the fabric, the higher the critical force and critical extension values are that follow linear tendencies with increasing stiffener concentration.

The critical shear angle has little dependence on the stiffness – it mainly depends on the fabric cell geometry that is not altered by the stiffener concentration.The critical shear angle increases negligibly with increasing stiffness, because stiffer fabric is able to support higher transverse compressive stresses before it buckles.

The image analysis system described was proved to be sensitive when supplying information about different fabric behaviour due to variations in the bending rigidity parameter, which influences post-buckling behaviour of fabric.

The repeatability of the results is greatly dependent on the maintenance of the same illumination conditions. The method gives a good representation of the out-of-plain deformation behaviour of bias cut specimens during uniaxial tension using relatively simple testing equipment.

Acknowledgments

We would like to thank Technical University of Liberec for assistance with the KES-FB testing, as part of project CoE-ITSAPT'2005.

References

1. *Mahar T.J., Ajiki I., Dhingra R.C., Postle R., Fabric Mechanical and Physical Properties Relevant to Clothing Manufacture – Part 3: Shape formation in Tailoring Int. J. of Cloth. Sc. and Tech. 1(3) 6-13, 1989.*
2. *Liu L., Chen J., Li X., Sherwood J., Two-dimensional macro mechanics shear models of woven fabrics Composites Part A: Applied Sc. and Manufacturing 36, 105-114, 2005.*
3. *Zheng J., Komatsu T., Yazaki Y., Takater, M., Inui S., Shimizu Y., Evaluating Shear Rigidity of Woven Fabrics Text. Res. J. 76 (2), 145-151, 2006.*
4. *Mohammed U., Lekakou C., Dong L., Bader M.G., Shear Deformation and Micromechanics of Woven Fabrics Composites Part A: Applied Sc. and Manufacturing 31, 299-308, 2000.*
5. *Potluri P., Ciurezu D.A.P., Ramgulam R.B., Measurement of Mesoscale Shear Deformations for modelling Textile Composites Composites Part A: Applied Sc. and Manufacturing 37, 303-314, 2006.*
6. *Kilby W.F., Planar Stress-Strain Relationships in Woven Fabrics J. Of the Text. Inst., 54, 9-27, 1963.*
7. *Amirbayat J., Alagha M.J., A New Approach to Fabric Assessment Int. J. of Cloth. Sc.and Tech. 7(1) 46-54, 2005.*
8. *Yick K.L., Chen, K.P.S., Dhingra R.C., How Y.L., Comparison of Mechanical Properties of Shirting Materials Measured on the KES-F and FAST Instruments Text. Res. J. 66 (10), 622-633, 1996.*
9. *Yu X., Cartwright B., McGuckin D., Ye L., Mai Y.W., Intra-ply Shear Locking In Finite Element Analyses of Woven Fabric Forming Process Composites Part A: Applied Sc. and Manufacturing 37, 790-803, 2006.*
10. *Alamdar-Yazdi A., A New Method to Evaluate Low-stress Shearing Behavior of Woven Fabrics Indian J. of Fibre & Text. Res. 29, 333-338, 2004.*
11. *Drobina R., Machnio M.S., Application of the Image Analysis Technique for Textile Identification AUTEX Res. J.6(1), 40-47, 2006.*
12. *Dobb B.M., Russell S.R., A System for the Quantitative Comparison of Wrinkling in Plain Fabrics J.Text.Inst. 86 (3), 495-497, 1995.*
13. *Domskienė J., Strazdienė E., Investigation of Fabric Shear Behavior Fibres and Text. in Eastern Europe 13(2(50)), 26-30, 2005.*
14. *Sidhu R.M.J.S., Averill R.C., Riaz M., Pourboghrat F., Finite Element Analysis of Textile Composite Preform Stamping Composite Structures 52, 483-497, 2001.*
15. *Harrison P., Clifford M.J., Long A.C., Shear Characterisation of Viscous Woven Textile Composites: a Comparisson Between Picture Frame and Bias Extension Experiments Composites Sc. and Tech. 64, 1453-1465, 2004.*
16. *Kawabata Evaluation System for Fabrics Manual, Kato Tech. Co. Ltd, Kyoto, Japan.*
17. *Zhu B., Yu T.X., Tao X.M., An Experimental Study of In-Plane Large Shear Deformation of Woven Fabric Composite Composites Sc. and Tech. 1-10, 2006.*

Received 8.01.2007 Reviewed 24.08.2008